ELSEVIER

International Journal of Solids and Structures 41 (2004) 1741–1752

INTERNATIONAL JOURNAL OF SOLIDS and STRUCTURES

www.elsevier.com/locate/ijsolstr

Semi-active damping of a clamped plate using PZT

Qirong Lin *, Paolo Ermanni

IMES-Strukturtechnologien, LEO C3.2, Leonhardstrasse 27, CH-8092 Zurich, Switzerland

Received 26 October 2003; received in revised form 26 October 2003

Abstract

Semi-active damping of a clamped plate using PZT with purely resistive circuit or resistive state-switched circuit is studied in this paper. The clamped plate bonded with PZT is modelled using Hamilton's principle and Galerkin's method. The optimal shunt resistance for the purely shunt resistive circuit together with the optimal placement of the PZT is investigated. For a resistive-state-switched circuit, Clark's control logic is employed to optimize the shunt resistance. Numerical simulations for these two systems are also presented. Furthermore, a negative capacitance is added to enhance the damping performance.

Keywords: Semi-active damping; Plate; PZT; Resistive; State-switched

1. Introduction

During the last two decades there has been increasing interest in vibration control using piezoelectric materials. Due to their direct and converse piezoelectric effect, they have been used extensively in active and/or passive ways. Recently attention was paid to the semi-passive damping because of its simple electronics. In semi-active damping arrangement, the power amplifiers, A/D- and D/A-converters and the microprocessor will not be needed any more so that it will be much easier to be integrated into the structure.

Hagood and von Flotow (1991) investigated the damping using the piezoelectric materials shunted with the passive electrical circuit. For resistive shunting, the piezoelectric materials will act in the way similar to viscoelastic materials. If shunted with a pair of resistor and inductor, the circuit can be tuned in a manner analogous to a mechanical vibration absorber. But only one mode vibration can be damped. Wu (1998) reported a method for passive piezoelectric shunt damping of multiple vibration modes using a single piezoelectric transducer. In that paper, a 'blocking' circuit, which consisted of one parallel capacitor–inductor anti-resonant circuit or a series of them, was employed in series with each parallel resistor–inductor shunt circuit designed for one structural mode. As piezoelectric materials exhibit variable mechanical stiffness between the open circuit and the close circuit, they can also be utilized for vibration control in the way of state-switching (Richard et al., 1999; Clark, 2000). Two of the early papers on the

* Corresponding author. Tel.: +41-163-36306; fax: +41-163-31125.
E-mail address: qqirong@sh163.net (Q. Lin).

0020-7683/$ - see front matter © 2003 Elsevier Ltd. All rights reserved.
doi:10.1016/j.ijsolstr.2003.11.023

vibration suppression by varying the stiffness were investigated by Chen (1984) and Onoda et al. (1990). In the work of Clark (2000), a semi-active control law was used to switch the electric shunt circuit of a piezoelectric actuator for energy dissipation. But only a very simple spring–mass system was demonstrated in that paper. To the author's knowledge, there are few papers dealing with vibration suppression of a plate structure using the resistive circuit or the state-switched circuit.

In this paper, semi-active damping of a one-dimensional beam structure using PZT with purely resistive circuit or resistive state-switched circuit is extended to a plate structure. A clamped plate is considered. Of note is that in a resistive-state-switched circuit, the system is switched between an open circuit and a resistive circuit. The model for a clamped plate bonded with PZT is built using Hamilton's principle and Galerkin's method. The optimal placement of the piezoelectric patch and the optimal shunting resistance for the purely shunt resistive circuit are presented. For a resistive-state-switched circuit, Clark's control logic is employed to optimize the shunting resistance. The comparison of these two kinds of circuit systems for semi-active damping is given together with the open circuit system and the circuit system that is state-switched between the open circuit and the short circuit in the numerical simulation. Furthermore, a negative capacitance is used to enhance the damping performance.

2. System model

Consider the system as shown in Fig. 1(a). A clamped plate is surface bonded with a piezoelectric patch. The piezoelectric patch is shunted with a purely resistive circuit, or a resistive-state-switched circuit. Further more a negative capacitance (Tang and Wang, 2001) is added to enhance the performance, as shown in Fig. 1(b). Using the Hamilton's principle, the mechanical and electrical equations of the system can be obtained as follows:

$$
\begin{aligned}
&(2\rho_s h_s + \rho_p h_p \Delta H)\frac{\partial^2 w}{\partial t^2} + \frac{E_s}{1-v_s^2} I_s \left(\frac{\partial^4 w}{\partial x^4} + 2\frac{\partial^4 w}{\partial x^2 \partial y^2} + \frac{\partial^4 w}{\partial y^4} \right) \\
&\quad + \frac{E_p}{1-v_p^2} I_p \left[\left(\frac{\partial^4 w}{\partial x^4} + 2\frac{\partial^4 w}{\partial x^2 \partial y^2} + \frac{\partial^4 w}{\partial y^4} \right) \Delta H + 2\left(\frac{\partial^3 w}{\partial x^3} + \frac{\partial^3 w}{\partial x \partial y^2} \right) \frac{\partial \Delta H}{\partial x} \right. \\
&\quad + 2\left(\frac{\partial^3 w}{\partial y^3} + \frac{\partial^3 w}{\partial x^2 \partial y} \right) \frac{\partial \Delta H}{\partial y} + 2(1-v_p)\frac{\partial^2 w}{\partial x \partial y}\frac{\partial^2 \Delta H}{\partial x \partial y} \\
&\quad \left. + \left(\frac{\partial^2 w}{\partial x^2} + v_p \frac{\partial^2 w}{\partial y^2} \right) \frac{\partial^2 \Delta H}{\partial x^2} + \left(\frac{\partial^2 w}{\partial y^2} + v_p \frac{\partial^2 w}{\partial x^2} \right) \frac{\partial^2 \Delta H}{\partial y^2} \right] \\
&\quad + h_{31} J_p \left[\frac{\partial^2}{\partial x^2}\left(D_p \Delta H \right) + \frac{\partial^2}{\partial y^2}\left(D_p \Delta H \right) \right] = f_w
\end{aligned}
\tag{1}
$$

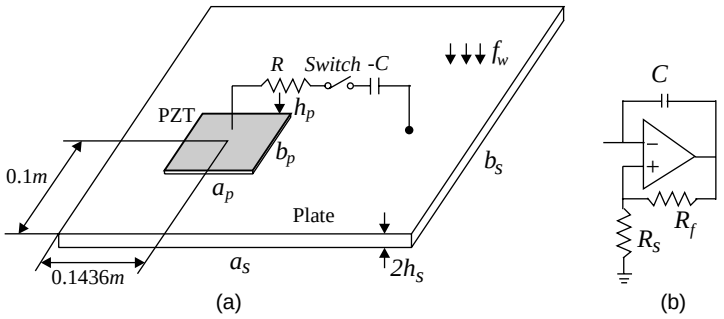

Fig. 1. (a) Cross-section of a beam with piezo patches; and (b) configuration of an aluminum beam bonded with a piezo patch.

$$V_{\mathrm{p}} - h_{31} J_{\mathrm{p}} \left(\frac{\partial^2 w}{\partial x^2} + \frac{\partial^2 w}{\partial y^2} \right) - \beta_{33} h_{\mathrm{p}} D_{\mathrm{p}} = 0 \tag{2}$$

where

$$I_{\mathrm{s}} = \tfrac{2}{3} h_{\mathrm{s}}^3, \qquad I_{\mathrm{p}} = \tfrac{1}{3}\left[(h_{\mathrm{s}} + h_{\mathrm{p}})^3 - h_{\mathrm{s}}^3 \right], \qquad J_{\mathrm{p}} = \tfrac{1}{2} h_{\mathrm{p}} (2h_{\mathrm{s}} + h_{\mathrm{p}}), \qquad A_{\mathrm{p}} = (x_{\mathrm{p2}} - x_{\mathrm{p1}})(y_{\mathrm{p2}} - y_{\mathrm{p1}}),$$

$$H = [H(x - x_{\mathrm{p1}}) - H(x - x_{\mathrm{p2}})] \cdot [H(y - y_{\mathrm{p1}}) - H(y - y_{\mathrm{p2}})]$$

w is the transverse displacement of the plate; D_{p} and V_{p} are respectively the electrical displacement of and the voltage on the piezoelectric patch; f_w is the external force applied on the plate; E_{s}, ρ_{s} , ν_{s} and h_{s} are, respectively, the Young's modulus, mass density, Poisson's ratio and half thickness of the plate; E_{p}, ρ_{p}, ν_{p}, h_{31}, β_{33} and h_{p} are the Young's modulus, mass density, Poisson's ratio, piezoelectric strain constant, piezoelectric dielectric constant and thickness of the piezoelectric patch, respectively; $H(\cdot)$ is unit Heaviside's function; $(x_{\mathrm{p1}}, y_{\mathrm{p1}})$ and $(x_{\mathrm{p2}}, y_{\mathrm{p2}})$ are, respectively, the corner coordinates of the piezoelectric patch.

Under the open circuit condition, the electrical displacement of the piezoelectric patch becomes zero and Eqs. (1) and (2) can be rewritten as:

$$\begin{aligned}
&(2\rho_{\mathrm{s}} h_{\mathrm{s}} + \rho_{\mathrm{p}} h_{\mathrm{p}} \Delta H) \frac{\partial^2 w}{\partial t^2} + \frac{E_{\mathrm{s}}}{1 - \nu_{\mathrm{s}}^2} I_{\mathrm{s}} \left(\frac{\partial^4 w}{\partial x^4} + 2 \frac{\partial^4 w}{\partial x^2 \partial y^2} + \frac{\partial^4 w}{\partial y^4} \right) \\
&\quad + \frac{E_{\mathrm{p}}}{1 - \nu_{\mathrm{p}}^2} I_{\mathrm{p}} \left[\left(\frac{\partial^4 w}{\partial x^4} + 2 \frac{\partial^4 w}{\partial x^2 \partial y^2} + \frac{\partial^4 w}{\partial y^4} \right) \Delta H + 2 \left(\frac{\partial^3 w}{\partial x^3} + \frac{\partial^3 w}{\partial x \partial y^2} \right) \frac{\partial \Delta H}{\partial x} \right. \\
&\quad + 2 \left(\frac{\partial^3 w}{\partial y^3} + \frac{\partial^3 w}{\partial x^2 \partial y} \right) \frac{\partial \Delta H}{\partial y} + 2(1 - \nu_{\mathrm{p}}) \frac{\partial^2 w}{\partial x \partial y} \frac{\partial^2 \Delta H}{\partial x \partial y} \\
&\quad \left. + \left(\frac{\partial^2 w}{\partial x^2} + \nu_{\mathrm{p}} \frac{\partial^2 w}{\partial y^2} \right) \frac{\partial^2 \Delta H}{\partial x^2} + \left(\frac{\partial^2 w}{\partial y^2} + \nu_{\mathrm{p}} \frac{\partial^2 w}{\partial x^2} \right) \frac{\partial^2 \Delta H}{\partial y^2} \right] = f_w
\end{aligned} \tag{3}$$

$$V_{\mathrm{p}} - h_{31} J_{\mathrm{p}} \left(\frac{\partial^2 w}{\partial x^2} + \frac{\partial^2 w}{\partial y^2} \right) = 0 \tag{4}$$

Note that Eq. (4) becomes the sensor equation for the open circuit.

For the short circuit, the voltage on the piezoelectric patch V_{p} is zero. Thus Eq. (1) becomes

$$\begin{aligned}
&(2\rho_{\mathrm{s}} h_{\mathrm{s}} + \rho_{\mathrm{p}} h_{\mathrm{p}} \Delta H) \frac{\partial^2 w}{\partial t^2} + \frac{E_{\mathrm{s}}}{1 - \nu_{\mathrm{s}}^2} I_{\mathrm{s}} \left(\frac{\partial^4 w}{\partial x^4} + 2 \frac{\partial^4 w}{\partial x^2 \partial y^2} + \frac{\partial^4 w}{\partial y^4} \right) \\
&\quad + \frac{E_{\mathrm{p}}}{1 - \nu_{\mathrm{p}}^2} I_{\mathrm{p}} \left[\left(\frac{\partial^4 w}{\partial x^4} + 2 \frac{\partial^4 w}{\partial x^2 \partial y^2} + \frac{\partial^4 w}{\partial y^4} \right) \Delta H + 2 \left(\frac{\partial^3 w}{\partial x^3} + \frac{\partial^3 w}{\partial x \partial y^2} \right) \frac{\partial \Delta H}{\partial x} \right. \\
&\quad + 2 \left(\frac{\partial^3 w}{\partial y^3} + \frac{\partial^3 w}{\partial x^2 \partial y} \right) \frac{\partial \Delta H}{\partial y} + 2(1 - \nu_{\mathrm{p}}) \frac{\partial^2 w}{\partial x \partial y} \frac{\partial^2 \Delta H}{\partial x \partial y} \\
&\quad \left. + \left(\frac{\partial^2 w}{\partial x^2} + \nu_{\mathrm{p}} \frac{\partial^2 w}{\partial y^2} \right) \frac{\partial^2 \Delta H}{\partial x^2} + \left(\frac{\partial^2 w}{\partial y^2} + \nu_{\mathrm{p}} \frac{\partial^2 w}{\partial x^2} \right) \frac{\partial^2 \Delta H}{\partial y^2} \right] \\
&\quad - \frac{(h_{31} J_{\mathrm{p}})^2}{h_{\mathrm{p}} \beta_{33}} \left[\frac{\partial^2}{\partial x^2} \left(\left(\frac{\partial^2 w}{\partial x^2} + \frac{\partial^2 w}{\partial y^2} \right) \Delta H \right) + \frac{\partial^2}{\partial y^2} \left(\left(\frac{\partial^2 w}{\partial x^2} + \frac{\partial^2 w}{\partial y^2} \right) \Delta H \right) \right] = f_w
\end{aligned} \tag{5}$$

If the piezoelectric patch is shunted with a circuit consisting of a resistor and a negative capacitor, Eqs. (1) and (2) become

$$\begin{aligned}
&\left(2\rho_s h_s + \rho_p h_p \Delta H\right)\frac{\partial^2 w}{\partial t^2} + \frac{E_s}{1-v_s^2} I_s \left(\frac{\partial^4 w}{\partial x^4} + 2\frac{\partial^4 w}{\partial x^2 \partial y^2} + \frac{\partial^4 w}{\partial y^4}\right) \\
&+ \frac{E_p}{1-v_p^2} I_p \left[\left(\frac{\partial^4 w}{\partial x^4} + 2\frac{\partial^4 w}{\partial x^2 \partial y^2} + \frac{\partial^4 w}{\partial y^4}\right)\Delta H + 2\left(\frac{\partial^3 w}{\partial x^3} + \frac{\partial^3 w}{\partial x \partial y^2}\right)\frac{\partial \Delta H}{\partial x}\right. \\
&+ 2\left(\frac{\partial^3 w}{\partial y^3} + \frac{\partial^3 w}{\partial x^2 \partial y}\right)\frac{\partial \Delta H}{\partial y} + 2(1-v_p)\frac{\partial^2 w}{\partial x \partial y}\frac{\partial^2 \Delta H}{\partial x \partial y} \\
&\left.+ \left(\frac{\partial^2 w}{\partial x^2} + v_p \frac{\partial^2 w}{\partial y^2}\right)\frac{\partial^2 \Delta H}{\partial x^2} + \left(\frac{\partial^2 w}{\partial y^2} + v_p \frac{\partial^2 w}{\partial x^2}\right)\frac{\partial^2 \Delta H}{\partial y^2}\right] \\
&- \frac{\left(h_{31} J_p\right)^2}{h_p \beta_{33}}\left[\frac{\partial^2}{\partial x^2}\left(\left(\frac{\partial^2 w}{\partial x^2} + \frac{\partial^2 w}{\partial y^2}\right)\Delta H\right)\right. \\
&\left.+ \frac{\partial^2}{\partial y^2}\left(\left(\frac{\partial^2 w}{\partial x^2} + \frac{\partial^2 w}{\partial y^2}\right)\Delta H\right)\right] \\
&+ \frac{\left(h_{31} J_p\right)^2}{h_p \beta_{33} A_p}\iint_{A_p}\left(\frac{\partial^2 w}{\partial x^2} + \frac{\partial^2 w}{\partial y^2}\right)\mathrm{d}x\,\mathrm{d}y \cdot \left(\frac{\partial^2 \Delta H}{\partial x^2} + \frac{\partial^2 \Delta H}{\partial y^2}\right) \\
&+ \frac{h_{31} J_p}{A_p}\left(\frac{\partial^2 \Delta H}{\partial x^2} + \frac{\partial^2 \Delta H}{\partial y^2}\right) Q_p = f_w
\end{aligned} \tag{6}$$

$$\left(R\frac{\mathrm{d}Q_p}{\mathrm{d}t} + \frac{1-\lambda}{C_p}Q_p + \frac{h_{31} J_p}{A_p}\iint_{A_p}\left(\frac{\partial^2 w}{\partial x^2} + \frac{\partial^2 w}{\partial y^2}\right)\mathrm{d}x\,\mathrm{d}y\right)\Delta H = 0 \tag{7}$$

where $C_p = \frac{A_p}{\beta_{33} h_p}$ and $Q_p = \int_{A_p} D_p \,\mathrm{d}x\,\mathrm{d}y$ are the equivalent capacitance of the piezoelectric patch and charge on the surface of the piezoelectric patch, respectively; λ is the ratio of the capacitance of the piezoelectric patch to the shunting negative capacitance; R is the resistance of the shunt circuit.

Galerkin's method is employed to discretize the above equations. The weighting function is chosen as the mode shape $\phi_{xi}(x)\phi_{yj}(y)$ of the clamped plate without shunted piezoelectric patches such that

$$w(x,y,t) = \sum_{i=1}^{n_x}\sum_{j=1}^{n_y}\phi_{xi}(x)\phi_{yj}(y)\eta_{ij}(t) \tag{8}$$

where $\eta_{ij}(t)$ is the generalized modal displacement, n_x and n_y are the expanding modes in x and y coordinates, respectively. The mode shape can be given in the form such that

$$\phi_{xi}(\bar{x}) = \alpha_i(\sin\beta_i\bar{x} - \gamma_i\cos\beta_i\bar{x} - \sinh\beta_i\bar{x} + \gamma_i\cosh\beta_i\bar{x}) \tag{9}$$

where

$$\begin{aligned}
\alpha_i &= \left(\gamma_i^2 - \frac{1-\gamma_i^2}{4\beta_i}\sin 2\beta_i - \frac{\gamma_i}{\beta_i}\sin^2\beta_i + \frac{1+\gamma_i^2}{4\beta_i}\sinh 2\beta_i + \frac{1-\gamma_i^2}{4\beta_i}\cos\beta_i\sinh\beta_i + 2\frac{\gamma_i}{\beta_i}\sin\beta_i\sinh\beta_i\right. \\
&\quad \left. - \frac{1+\gamma_i^2}{\beta_i}\sin\beta_i\cosh\beta_i - \frac{\gamma_i}{\beta_i}\sinh^2\beta_i\right)^{-1/2}, \\
\gamma_i &= \frac{\sin\beta_i - \sinh\beta_i}{\cos\beta_i - \cosh\beta_i}, \qquad \cos\beta_i\cosh\beta_i = 1, \qquad \bar{x} = \frac{x}{a_s}
\end{aligned}$$

Here a_s is the length of the plate and its width is denoted by b_s. $\phi_{yj}(y)$ is similar to $\phi_{xj}(x)$ in the form and is omitted here.

Thus Eqs. (3), (5) and (6) can be discretized as in the following form:

$$M\ddot{\eta} + C_b\dot{\eta} + K\eta + K_C Q_p = Ff_{wt} \tag{10}$$

where

$$M_{mnij} = 2\rho_s h_s a_s b_s \delta_{mi}\delta_{nj} + \rho_p h_p \int_{x_{p1}}^{x_{p2}} \phi_{xm}\phi_{xi}\,dx \int_{y_{p1}}^{y_{p2}} \phi_{yn}\phi_{yj}\,dy$$

$K_{mnij} = K^{oc}_{mnij}$ under the open circuit condition

$K_{mnij} = K^{sc}_{mnij}$ under the short circuit condition

$K_{mnij} = K^{rc}_{mnij}$ under the shunt resistive circuit condition

$$\begin{aligned}
K^{oc}_{mnij} = {} & \frac{E_s}{1-\nu_s^2} I_s \left(\beta_i^4 \delta_{mi}\delta_{nj} + 2\int_0^{a_s} \phi_{xm}\frac{\partial^2\phi_{xi}}{\partial x^2}dx \int_0^{b_s} \phi_{yn}\frac{\partial^2\phi_{yj}}{\partial y^2}dy + \beta_j^4\delta_{mi}\delta_{nj} \right) \\
& + \frac{E_p}{1-\nu_p^2} I_p \left[\int_{x_{p1}}^{x_{p2}} \phi_{xm}\frac{\partial^4\phi_{xi}}{\partial x^4}dx \int_{y_{p1}}^{y_{p2}} \phi_{yn}\phi_{yj}dy + 2\int_{x_{p1}}^{x_{p2}} \phi_{xm}\frac{\partial^2\phi_{xi}}{\partial x^2}dx \int_{y_{p1}}^{y_{p2}} \phi_{yn}\frac{\partial^2\phi_{yj}}{\partial y^2}dy \right. \\
& + \int_{x_{p1}}^{x_{p2}} \phi_{xm}\phi_{xi}dx \int_{y_{p1}}^{y_{p2}} \phi_{yn}\frac{\partial^4\phi_{yj}}{\partial y^4}dy + \left(\frac{\partial\phi_{xm}}{\partial x}\frac{\partial^2\phi_{xi}}{\partial x^2} - \phi_{xm}\frac{\partial^3\phi_{xi}}{\partial x^3} \right)\Bigg|_{x_{p1}}^{x_{p2}} \int_{y_{p1}}^{y_{p2}} \phi_{yn}\phi_{yj}dy \\
& + \left((\nu_p - 2)\phi_{xm}\frac{\partial\phi_{xi}}{\partial x} + \nu_p\phi_{xi}\frac{\partial\phi_{xm}}{\partial x} \right)\Bigg|_{x_{p1}}^{x_{p2}} \int_{y_{p1}}^{y_{p2}} \phi_{yn}\frac{\partial^2\phi_{yj}}{\partial y^2}dy + \left(\frac{\partial\phi_{yn}}{\partial y}\frac{\partial^2\phi_{yj}}{\partial y^2} - \phi_{yn}\frac{\partial^3\phi_{yj}}{\partial y^3} \right)\Bigg|_{y_{p1}}^{y_{p2}} \int_{x_{p1}}^{x_{p2}} \phi_{xm}\phi_{xi}dx \\
& + \left((\nu_p - 2)\phi_{yn}\frac{\partial\phi_{yj}}{\partial y} + \nu_p\phi_{yj}\frac{\partial\phi_{yn}}{\partial y} \right)\Bigg|_{y_{p1}}^{y_{p2}} \int_{x_{p1}}^{x_{p2}} \phi_{xm}\frac{\partial^2\phi_{xi}}{\partial x^2}dx \\
& \left. + 2(1-\nu_p)\left(\phi_{xm}\frac{\partial\phi_{xi}}{\partial x} \right)\Bigg|_{x_{p1}}^{x_{p2}} \left(\phi_{yn}\frac{\partial\phi_{yj}}{\partial y} \right)\Bigg|_{y_{p1}}^{y_{p2}} \right]
\end{aligned}$$

$$\begin{aligned}
K^{sc}_{mnij} = {} & K^{oc}_{mnij} - \frac{\left(h_{31}J_p\right)^2}{h_p\beta_{33}} \left[\int_{x_{p1}}^{x_{p2}} \phi_{xm}\frac{\partial^4\phi_{xi}}{\partial x^4}dx \int_{y_{p1}}^{y_{p2}} \phi_{yn}\phi_{yj}dy + 2\int_{x_{p1}}^{x_{p2}} \phi_{xm}\frac{\partial^2\phi_{xi}}{\partial x^2}dx \int_{y_{p1}}^{y_{p2}} \phi_{yn}\frac{\partial^2\phi_{yj}}{\partial y^2}dy \right. \\
& + \int_{x_{p1}}^{x_{p2}} \phi_{xm}\phi_{xi}dx \int_{y_{p1}}^{y_{p2}} \phi_{yn}\frac{\partial^4\phi_{yj}}{\partial y^4}dy + \left(\frac{\partial\phi_{xm}}{\partial x}\frac{\partial^2\phi_{xi}}{\partial x^2} - \phi_{xm}\frac{\partial^3\phi_{xi}}{\partial x^3} \right)\Bigg|_{x_{p1}}^{x_{p2}} \int_{y_{p1}}^{y_{p2}} \phi_{yn}\phi_{yj}dy \\
& + \left(\phi_{xi}\frac{\partial\phi_{xm}}{\partial x} - \phi_{xm}\frac{\partial\phi_{xi}}{\partial x} \right)\Bigg|_{x_{p1}}^{x_{p2}} \int_{y_{p1}}^{y_{p2}} \phi_{yn}\frac{\partial^2\phi_{yj}}{\partial y^2}dy + \left(\frac{\partial\phi_{yn}}{\partial y}\frac{\partial^2\phi_{yj}}{\partial y^2} - \phi_{yn}\frac{\partial^3\phi_{yj}}{\partial y^3} \right)\Bigg|_{y_{p1}}^{y_{p2}} \int_{x_{p1}}^{x_{p2}} \phi_{xm}\phi_{xi}dx \\
& \left. + \left(\phi_{yj}\frac{\partial\phi_{yn}}{\partial y} - \phi_{yn}\frac{\partial\phi_{yj}}{\partial y} \right)\Bigg|_{y_{p1}}^{y_{p2}} \int_{x_{p1}}^{x_{p2}} \phi_{xm}\frac{\partial^2\phi_{xi}}{\partial x^2}dx \right]
\end{aligned}$$

$$K^{\mathrm{rc}}_{mnij} = K^{\mathrm{sc}}_{mnij} + \frac{\left(h_{31}J_{\mathrm{p}}\right)^2}{h_{\mathrm{p}}\beta_{33}A_{\mathrm{p}}}\left[\frac{\partial\phi_{xi}}{\partial x}\Big|_{x_{\mathrm{p1}}}^{x_{\mathrm{p2}}}\int_{y_{\mathrm{p1}}}^{y_{\mathrm{p2}}}\phi_{yj}\,\mathrm{d}y + \frac{\partial\phi_{yj}}{\partial y}\Big|_{y_{\mathrm{p1}}}^{y_{\mathrm{p2}}}\int_{x_{\mathrm{p1}}}^{x_{\mathrm{p2}}}\phi_{xi}\,\mathrm{d}x\right] \times\left[\frac{\partial\phi_{xm}}{\partial x}\Big|_{x_{\mathrm{p1}}}^{x_{\mathrm{p2}}}\int_{y_{\mathrm{p1}}}^{y_{\mathrm{p2}}}\phi_{yn}\,\mathrm{d}y + \frac{\partial\phi_{yj}}{\partial y}\Big|_{y_{\mathrm{p1}}}^{y_{\mathrm{p2}}}\int_{x_{\mathrm{p1}}}^{x_{\mathrm{p2}}}\phi_{xm}\,\mathrm{d}x\right]$$

$K_{Cmn} = 0$ under the open or short circuit conditions

$$K_{Cmn} = \frac{h_{31}J_{\mathrm{p}}}{A_{\mathrm{p}}}\left[\frac{\partial\phi_{xm}}{\partial x}\Big|_{x_{\mathrm{p1}}}^{x_{\mathrm{p2}}}\int_{y_{\mathrm{p1}}}^{y_{\mathrm{p2}}}\phi_{yn}\,\mathrm{d}y + \frac{\partial\phi_{yj}}{\partial y}\Big|_{y_{\mathrm{p1}}}^{y_{\mathrm{p2}}}\int_{x_{\mathrm{p1}}}^{x_{\mathrm{p2}}}\phi_{xm}\,\mathrm{d}x\right]$$ under the shunt resistive circuit condition

$$C_{bmnij} = c_b\delta_{mi}\delta_{nj}$$

$$F_{mn} = \int_{x_{\mathrm{p1}}}^{x_{\mathrm{p2}}}\int_{y_{\mathrm{p1}}}^{y_{\mathrm{p2}}} f_{wx}(x)\phi_{xm}\phi_{yn}\,\mathrm{d}x\,\mathrm{d}y$$

$$f_w(x,t) = f_{wx}(x)f_{wt}(t)$$

Note that a viscous damping term $C_b\dot{\eta}$ is added in Eq. (10), and c_b is the damping coefficient.

Under the open circuit condition, the charge on the patch can be obtained from Eq. (4) as follows:

$$Q_{\mathrm{p}} = C_{\mathrm{p}}K_c\eta \tag{11}$$

The electrical equation (7) under the resistive circuit condition can be discretized as:

$$R\frac{\mathrm{d}Q_{\mathrm{p}}}{\mathrm{d}t} + \frac{1-\lambda}{C_{\mathrm{p}}}Q_{\mathrm{p}} + K_c\eta \tag{12}$$

The piezo patch introduces higher stiffness in the system when it is under open circuit condition than when it is short-circuited. When the piezo patch is shunted with a resistive circuit, the stiffness of the piezo patch is also related to the shunt resistance and negative capacitance. It is intuitively clear that the stiffness of the resistive circuit system is between the short circuit system and the open circuit system.

3. Optimal placement of PZT and resistance for the purely resistive shunt circuit

The mechanical equation (10) and the electrical equation (12) under the purely resistive shunt circuit can be cast in the state space form as

$$\dot{x} = Ax + Bf_{wt} \tag{13}$$

$$y = Cx \tag{14}$$

where

$$x = [\,\eta \quad \dot{\eta} \quad Q_{\mathrm{p}}\,]^{\mathrm{T}}, \qquad y = w(x_{\mathrm{s}}, y_{\mathrm{s}}, t), \qquad A = \begin{bmatrix} 0 & I & 0 \\ -M^{-1}K & -M^{-1}C_b & -M^{-1}K_C \\ -R^{-1}K_C^{\mathrm{T}} & 0 & -\frac{1-\lambda}{RC_{\mathrm{p}}} \end{bmatrix},$$

$$B = \begin{bmatrix} 0 & M^{-1}F & 0 \end{bmatrix}^{\mathrm{T}}, \qquad C = [\,\phi_{x1}(x_{\mathrm{s}})\phi_{y1}(y_{\mathrm{s}})\cdots\phi_{xi}(x_{\mathrm{s}})\phi_{yj}(y_{\mathrm{s}}) \quad 0 \quad 0\,]$$

Note that the output is the deflection at the specific point (x_s, y_s) in the plate. The optimal placement of the PZT and the optimal shunt resistance for the resistive circuit will be found to minimize the following objective function, which is chosen as the norm of the continuous system's transfer function:

$$J = \|C(Is - A)^{-1}B\|_2 \tag{15}$$

4. Optimal resistance for the resistive-state-switched circuit

For the resistive-state-switched circuit system, the control law by Clark (2000) is adopted here. When the defection and velocity at the specific point (x_s, y_s) in the plate satisfy

$$w(x_s, y_s, t)\dot{w}(x_s, y_s, t) \geqslant 0 \tag{16}$$

the circuit will be switched to the open circuit. Or else it will be switched to the closed circuit. Since the resistive-state-switched circuit system is nonlinear, the optimal resistance in the circuit will be found to minimize the following objective function similar to that by Clark (2000):

$$J = \int_0^{t_f} |w(x_s, y_s, t)| \, \mathrm{d}t \tag{17}$$

5. Numerical simulation for impulse response

Consider the configuration of a clamped plate bonded with the PZT as shown in Fig. 1(a). The system parameters are listed in Table 1. In the following numerical examples, only the first two modes of the clamped plate are considered such that $n_x = 2$, $n_y = 1$. An impulse force

$$f_w(x, y, t) = \delta(x - x_s)\delta(y - y_s)\delta(t) \tag{18}$$

is applied at the specific point $(x_s = 0.4a_s, y_s = 0.4b_s)$ in the plate to determine the optimal placement of the PZT and the optimal resistance for purely resistive circuit system and the resistive-state-switched circuit system. The optimal placement of the PZT is found that its center should be located at the point $(0.1436 \text{ m}, 0.1 \text{ m})$. The optimal resistance with the optimal placement is 2225.5 Ω for the purely resistive circuit system by minimizing the objective function 15, while it is only 525.4 Ω for the resistive state-switched circuit system by minimizing the objective function 17. Of note is that the placement of the PZT for the resistive-state-switched circuit system is not optimized and is kept as that in the purely resistive circuit. It shows that the resistive-state-switched circuit system needs much less resistance than the purely resistive circuit system. The objective functions for these two systems are shown in Figs. 2 and 3. The comparison of the frequency responses of the open circuit system and the purely resistive circuit system is shown in Fig. 4.

Table 1
System parameters

$a_s = 0.35$ m	$v_s = 0.3$
$b_s = 0.20$ m	$c_b = 0.12$ N s/m^2
$h_s = 0.0005$ m	$E_p = 59$ GPa
$a_p = 0.35$ m	$\rho_p = 7600$ kg/m^3
$b_p = 0.20$ m	$v_p = 0.35$
$h_p = 0.0005$ m	$h_{31} = 7.664 \times 10^8$ N/C
$E_s = 71$ GPa	$\beta_{33} = 7.331 \times 10^7$ V m/C
$\rho_s = 2906$ kg/m^3	$\lambda = 0.9$

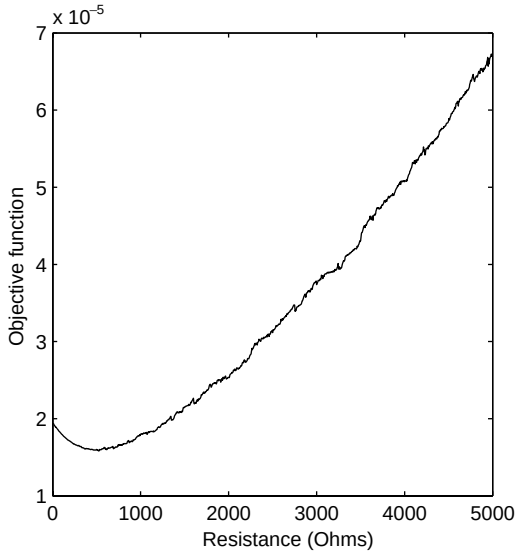

Fig. 2. Objective function for the resistive state-switched circuit system.

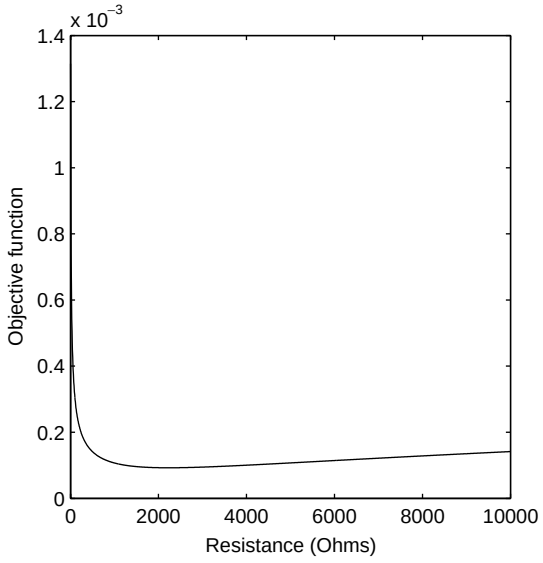

Fig. 3. Objective function for the resistive circuit system.

After the optimal placement of PZT and the optimal resistance are determined, the impulse responses of these two systems are simulated together with the open to short circuit state-switched system and the open circuit system. Note that in the purely resistive circuit system and the resistive-state-switched circuit system, a negative capacitance ($\lambda = 0.9$) is added to enhance the damping performance. Fig. 5 shows the impulse responses at the specific point (x_s, y_s) in the plate for the purely resistive circuit system and the resistive state-switched circuit system. Although the performance of the resistive-state-switched circuit is not better

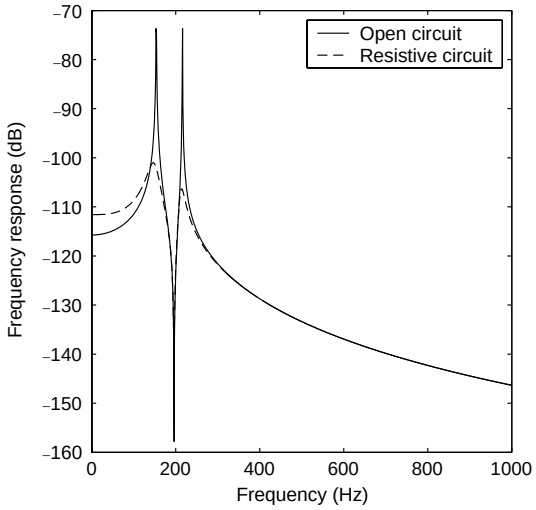

Fig. 4. Frequency response at the point $(0.4a_s, 0.4b_s)$.

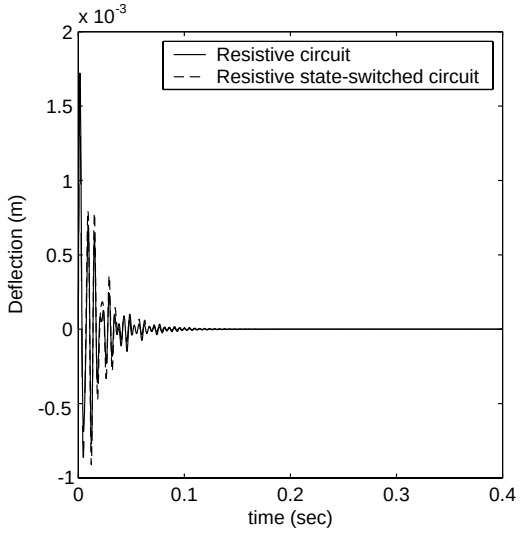

Fig. 5. Impulse responses at the point $(0.4a_s, 0.4b_s)$ for the systems with a negative capacitance.

than the purely resistive circuit in the above numerical simulation, one should note that the resistance needed for the resistive state-switched circuit is much less than that in the purely resistive circuit. Furthermore, the resistive-state-switched circuit may be more robust than the purely resistive circuit. This is due to the fact that the piezoelectric capacitance is nonlinear in practice and dependent on the frequency. The impulse responses at the specific point for the open circuit and the open to short circuit state-switched are given in Fig. 6. It shows that the vibration of the plate can also be damped somewhat by state-switching between the open and short circuit. If no negative capacitance is added in the circuit, the optimal resistances

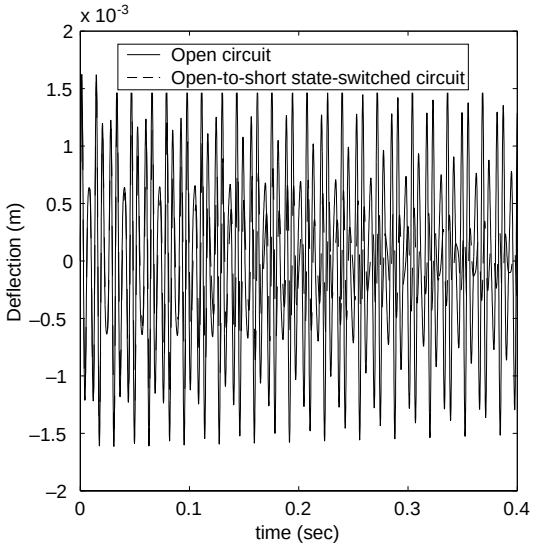

Fig. 6. Impulse responses at the point $(0.4a_s, 0.4b_s)$.

for the purely resistive circuit system and the resistive-state-switched circuit system are respectively 17,887 and 2362.5 Ω, which are much larger than the ones with the negative capacitance. Fig. 7 shows the impulse responses for these two systems without the negative capacitance. It can be seen by comparison of Figs. 5 and 7 that adding a negative capacitance can greatly improve the damping performance of the purely resistive circuit system and the resistive-state-switched circuit system. From the impulse response of the state-switched circuit system with and without a resistor, as shown in Figs. 5–7, it can also be seen that the switch damping performance can be improved by introducing a resistor in the circuit, especially together

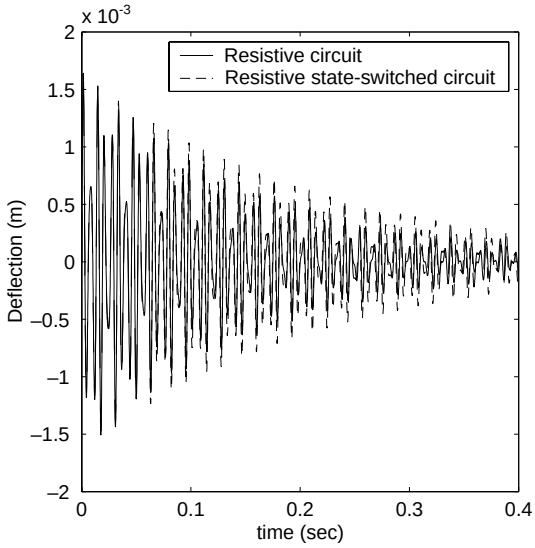

Fig. 7. Impulse responses at the point $(0.4a_s, 0.4b_s)$ for the systems without a negative capacitance.

with a negative capacitor. The charges on the piezoelectric patch for all the above circuit systems are shown in Figs. 8–10. In fact the damping performance can also be judged from the charge on the piezoelectric patch. It can be seen by comparison of Figs. 8 and 10 that adding a negative capacitance can increase the energy transfer of the mechanical vibration energy into the electrical energy and thus increase the system damping.

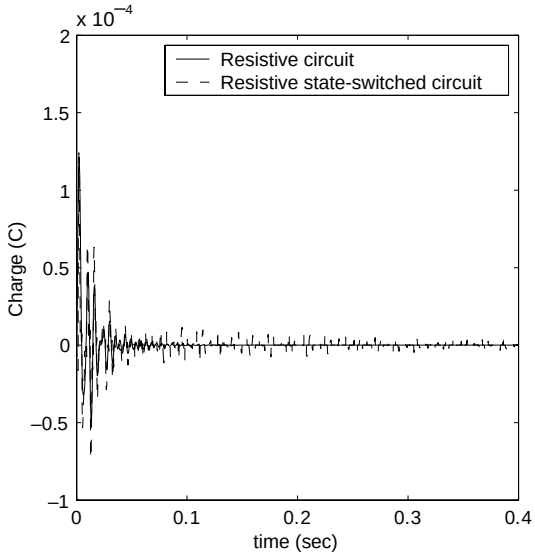

Fig. 8. Charge on the piezoelectric patch for the system with a negative capacitance.

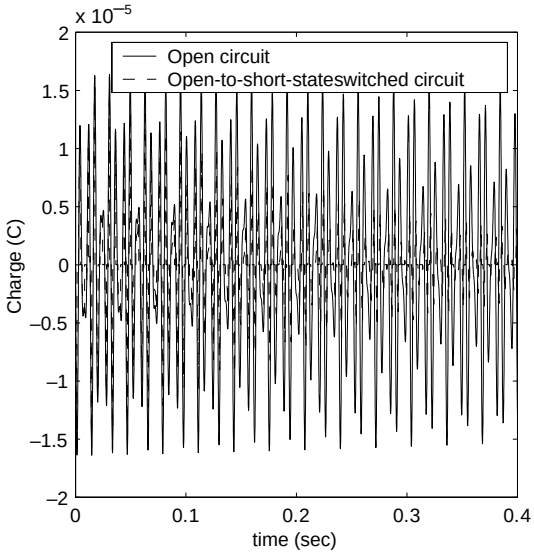

Fig. 9. Charge on the piezoelectric patch.

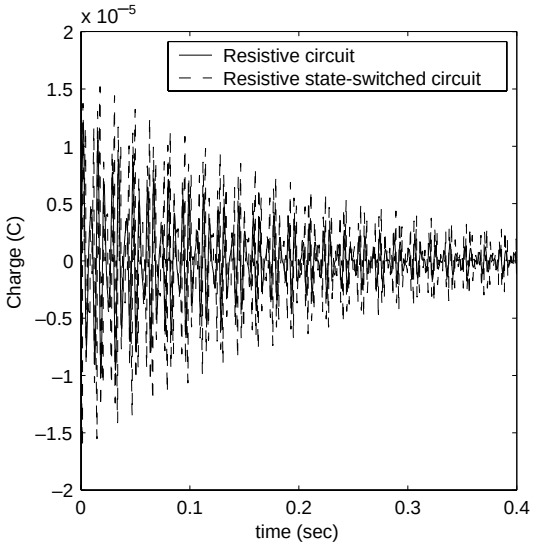

Fig. 10. Charge on the piezoelectric patch for the system without a negative capacitance.

6. Conclusion

The semi-active damping using PZT with the purely resistive circuit or the resistive state-switched circuit is investigated in this paper. A two-dimensional plate structure is modelled. In most previous papers on semi-active damping, the placement of the piezoelectric patch is rarely optimized. There should be a compromise between the shunt resistance and the placement of the piezoelectric patch regarding the modes to be controlled. For a plate structure, the optimal length and width of the shunted piezoelectric patched is also correlated with each other. The resistance for the circuit system together with the placement of the piezoelectric patch is optimized herein. The damping performance of different circuit systems is numerically simulated. Results demonstrate that adding a negative capacitance can significantly increase the damping for the purely resistive circuit system and the resistive-state-switched circuit system. It seems that the resistive-state-switched circuit system cannot outperform the purely resistive circuit system in the simulation. But it should be noted that the piezoelectric capacitance is nonlinear in practice and dependent on the frequency. Thus the purely resistive circuit may be not so robust as the resistive-state-switched circuit system.

References

Chen, J.C., 1984. Response of large space structures with stiffness control. Journal of Spacecraft and Rockets 21 (5), 463–467.

Clark, W.W., 2000. Vibration control with state-switched piezoelectric materials. Journal of Intelligent Material Systems and Structures 11, 263–271.

Hagood, N.W., von Flotow, A., 1991. Damping of structural vibrations with piezoelectric materials and passive networks. Journal of Sound and Vibration 146 (2), 243–268.

Onoda, J., Endo, T., Tamaoki, T.H., Watanabe, N., 1990. Vibration suppression by variable-stiffness members. In: 31st AIAA/ASME/ASCE/AHS/ASC Structures, Structural Dynamics and Materials Conference. AIAA, New York, USA, pp. 2359–2366.

Richard, C., Guyomar, D., Audigier, D., Ching, G., 1999. Semi-passive damping using continuous switching of a piezoelectric device. In: Proceedings of SPIE Conference on Passive Damping and Isolation, 3672. SPIE, California, USA, pp. 104–111.

Tang, J., Wang, K.W., 2001. Active-passive hybrid piezoelectric networks for vibration control: comparisons and improvement. Smart Materials and Structures 10 (4), 794–806.

Wu, S.Y., 1998. Method for multiple-mode shunt damping of structural vibration using a single PZT transducer. In: Proceedings of SPIE Smart Structures and Materials: passive damping and isolation, 3327. SPIE, San Diego, USA, pp. 159–168.